Evaluation of using absolute vs. relative base level when analyzing brain activation images using the scale-space primal sketch[*]

Mikael Rosbacke[1], *Tony Lindeberg*[1] and *Per E. Roland*[2]

[1]Computational Vision and Active Perception Laboratory (CVAP)
Dept. of Numerical Analysis and Computing Science (NADA)
KTH (Royal Institute of Technology)
S-100 44 Stockholm, Sweden
{rosbacke, tony}@nada.kth.se

[2]Division of Human Brain Research
Department of Neuroscience
Karolinska Institutet, S-171 77 Solna, Sweden
per.roland@neuro.ki.se

Abstract

A dominant approach to brain mapping is to define functional regions in the brain by analyzing images of brain activation obtained from positron emission tomography (PET) and functional magnetic resonance imaging (fMRI). This paper presents an evaluation of using one such tool, called the scale-space primal sketch, for brain activation analysis. A comparison is made concerning two possible definitions of the scale-space significance measure, where local contrast is measured either relative to a local or global reference level.

Experiments on real brain data show that the global approach with absolute base level gives a higher significance to small blobs superimposed on larger scale structures, than a local approach with relative base level, whereas the significance of isolated blobs largely remains unaffected. The global approach also has a higher degree of correspondence to a traditional statistical method.

Relative to previously reported works, the following two technical improvements are also presented: (i) A post-processing tool is introduced for merging multiple blob responses to similar image structures. This simplifies automated analysis from the scale-space primal sketch. (ii) A new approach is introduced for scale-space normalization of the significance measure, by collecting reference statistics of residual noise images obtained from the general linear model.

Keywords: brain activation, brain mapping, functional region, scale-space, primal sketch

1   Introduction

In functional brain imaging, one studies neuronal activity of the brain when subjects perform different tasks. A main purpose is to characterize functional regions activated in the cerebral cortex. Two main goals in this context are to localize the regions of interest and to measure the level of activity. The underlying hypothesis to this approach is that neurons are activated in large populations, also known as the cortical field activation hypothesis (Roland, 1993). The two most common imaging techniques used today are PET and fMRI, and a large number of techniques have been developed to analyze such data. In this paper, we focus mainly on images derived from PET studies, where one relies on the tight spatial coupling between neuronal activity and local cerebral blood flow.

Previous works on detecting functional regions have been done with different statistical approaches. (Friston et al., 1991), (Friston et al., 1994), (Worsley et al., 1992), (Worsley et al., 1996b) use the theory of Gaussian random fields to derive a probability measure of the activations in PET images. (Holmes et al., 1996) suggest a non-parametric approach with permutations in the ordering of PET images to derive a probability measure. (Poline and Mazoyer, 1993), (Roland et al., 1993), (Ledberg et al., 1999) uses noise images from PET experiments to generate synthetic noise images, to derive a probability distribution in a Monte Carlo fashion.

In this paper, we will use a tool from the computer vision community, called the scale-space primal sketch. It is based on scale-space theory (Witkin, 1983), (Koenderink, 1984), (Lindeberg, 1994), (Florack, 1997) and has been proposed as a method for PET image analysis by (Lidberg et al., 1996), (Coulon et al., 1996), (Coulon et al., 1997) and (Lindeberg et al., 1999). Some attractive properties of this method are that it only makes few assumptions on the data, there is no need for determining the amount of spatial filtering and the process for extracting regions of interest is fully automatic.

Aim of paper. The aim of this paper is to investigate a modification of the scale-space primal sketch approach. In the original method, the regions of interest were ranked according to significance by measuring the volumes that certain primitives, called scale-space blobs, occupy in scale-space. These scale-space blobs do not constitute a significance measure in the statistical sense, since no p-value is attached to each scale-space blob. In the following, the term significance will mean the scale-space primal sketch significance unless otherwise stated.

The scale-space primal sketch was originally developed to deal with natural images, in which brightness variations are judged from relative comparisons and for which there is no absolute reference level to which intensity differences can be related. This made it natural to base the significance measure on a relative base level, measuring the intensities of the blobs from the base level of a so-called delimiting saddle point of the blob (defined in section 2.3). On the other hand, when analyzing statistical contrast images, as obtained by fitting a general linear model to the data, there is a preferred statistically determined absolute zero level. For this reason, one may consider an alternative approach of defining the local contrast of blobs relative to an absolute base level (see section 2.3.2).

In our method, the PET images are realigned, reformatted to standard anatomical format (Roland et al., 1994) and a general linear model is used. From the linear model, student-t test images are derived from contrast images, which represent the contrast between two experimental conditions. Since the mean value of a voxel across all the PET images is excluded from the contrast, the global zero-level of the contrast signifies a border between the two included test conditions. All values above the zero

level represent a higher activation in the first condition and values below zero a higher activation in the second condition. This paper will investigate the effect of using an absolute base level in the scale-space primal sketch, in order to relate the volume of the scale-space blobs to a global zero level.

Merging of multiple responses. During the work with the scale-space primal sketch it has been noted that several blobs may be extracted corresponding to the same underlying activation. The division of the activation among several scale-space blobs has the effect of dividing the significance measure among these blobs and the ranking will not reflect the underlying strength of the activation. To reduce this effect, a method will be proposed to identify this type of scale-space blob fragmentation and to merge these scale-space blobs together to form a new blob, which better represents the underlying activation (see section 3.2).

Estimation of statistical properties from blobs using residual noise. The scale-space primal sketch needs an estimation of the statistical distribution of grey-level blobs across scales in order to properly assign significance measures to the brain activations. In previous works, this statistics has been collected from reference images, which have been either generated from white noise images (Lindeberg 1993) or difference images, alternatively student-t images, from PET experiments.

In this work, we will also make use of a new approach for generating reference statistics for scale normalization. The idea is to use residual images as obtained from the general linear model used as a pre-processing stage to the scale-space analysis. Preliminary results by (Björkman et al., 1999) demonstrate that this model has attractive properties for separating blobs representing brain activations in PET images from blobs extracted from noise patterns.

2 Theory

The scale-space primal sketch is a representation developed to extract blob structures in image data. In this section, we will give a brief review of the theory of the general linear model, scale-space representation and the scale-space primal sketch.

2.1 Brief review of the general linear model

The general linear model (Searle, 1971) is used for inter-subject averaging and decomposition of the images into different test conditions. This is done by applying a linear model for every voxel. Each PET-image is usually classified according to which test subject it represents and which test condition was performed during the image acquisition. Each subject and each condition in the experiment is assigned an unknown parameter in the experiment and an additional parameter is assigned for the mean value of each voxel. The parameters are connected to the PET images by a set of explanatory variables, which indicate when a PET image belongs to a certain test subject and test condition.

Let $v_n(x)$ denote the voxel intensity of PET image $n \in [1,\, N]$ at position $x = (x_1, x_2, x_3)^T$. The different test subjects and test conditions are assigned unknown parameters $\beta_j(x)$ where $j \in [1,\, J]$ and $\beta_0(x)$ is the mean intensity value at every voxel x over the PET images. Let $z_{jn} \in \{0,\, 1\}$ be the explanatory variables which connect PET image n to the unknown parameter β_j. Every PET image is usually connected to one test subject and one test condition and z_{jn} is set to 1 at these positions, otherwise 0. (The rest condition is considered a test condition in this context.) The vector z_{0n}

has the value 1 for $n \in [1, N]$ such that $\beta_0(x)$ represents the mean value of voxel x and the remaining residual noise in the model is modeled by $\varepsilon_n(x)$. The model can then be written in matrix form as

$$V(x) = Z\beta(x) + \varepsilon(x) \tag{1}$$

where $V(x) = [v_1(x), ..., v_n(x)]^T$, $\beta(x) = [\beta_0(x), ..., \beta_J(x)]^T$, $\varepsilon(x) = [\varepsilon_1(x), ..., \varepsilon_n(x)]^T$ and Z is a design matrix of size $N \times (J + 1)$. This model is applied for every voxel x in the PET-images and is solved for the unknowns $\beta(x)$.

This model is generally overdetermined, and the solution is obtained by minimizing of the squared residual sum $\varepsilon(x)^T \varepsilon(x)$ of the model, also known as a least square fit of the model. If the design matrix Z is of full rank, this is done by the solution $\beta(x) = (Z^T Z)^{-1} Z^T V(x)$ of the normal equation. However, the design matrix of PET experiments is usually not of full rank and a generalized inverse C which satisfies $(Z^T Z)C(Z^T Z) = Z^T Z$, is used for the solution. A linear subspace remains undetermined by this approach and we arbitrarily choose one instance of the free subspace and the solution, denoted by

$$\beta(x) = CZ^T V(x) \tag{2}$$

To perform a test on the data, a *contrast image* is derived from the $\beta(x)$ parameters. A column vector w of length $(J + 1)$ is constructed to represent this contrast in such a way that the contrast image is not dependent on the free subspace. A safe way to construct the w vector is to decompose it into three blocks corresponding to the mean value, the test conditions and the test subjects. If the sum of the components in each block of w is zero, then it is properly constructed. The contrast image $c(u)$ is then derived from w by

$$c(x) = w^T \beta(x) \; \forall x \tag{3}$$

The student-t statistical image used for the actual test is formed by the contrast image according to

$$f(x) = \frac{c(x)}{\sqrt{var[c(x)]}} \tag{4}$$

where the variance $var[c(x)]$ is computed as

$$var[c(x)] = w^T CZ^T ZC^T w\sigma^2 \tag{5}$$

where σ^2 is the variance of the noise estimated as

$$\sigma^2 = \frac{1}{v} V^T(x)(I - ZCZ^T)V(x) \tag{6}$$

and $v = N - rank(Z)$ is the number of degrees of freedom of the test. These are the image data that will be analyzed by the scale-space analysis described in the next section.

2.2 Scale-space representation

The scale-space representation $L : R^D \times R_+ \to R$ for a D-dimensional image $f : R^D \to R$ is constructed by adding one dimension representing scale changes. L is defined such that the original image corresponds to the zero level in the scale-space representation

$$L(\cdot; 0) = f(\cdot) \tag{7}$$

and coarser scale representations for $t > 0$ are obtained by convolution

$$L(\cdot; t) = g(\cdot; t) \star f(\cdot) \tag{8}$$

with the Gaussian kernel

$$g(x;t) = \frac{1}{(2\pi t)^{D/2}} e^{-x^T x/2t} \tag{9}$$

As the scale parameter increases, the images at the corresponding scale are smoothed and structures with size corresponding to the smoothing kernel may be detected at that scale level. The choice of the Gaussian kernel can be shown to be unique, given natural symmetry requirements referred to as scale-space axioms. For a more thorough discussion of scale-space theory, see (Witkin, 1983), (Koenderink, 1984), (Lindeberg, 1994) or (Florack, 1997).

2.3   The scale-space primal sketch

The scale-space primal sketch is a representation which makes an explicit description of an image in scale-space, in terms of extremum points and their surroundings, also referred to as grey-level blobs. The grey-level blobs impose a boundary between regions of interest and background and are linked across scales in a hierarchical fashion to form a hierarchy of scale-space blobs. We will here give a brief review. For a more thorough description, see (Lindeberg, 1993), (Lindeberg et al., 1999).

2.3.1   Grey-level blobs

A grey-level blob is defined at a single scale and represents a local intensity extremum point P_e at a given scale t with a surrounding spatial support region, delimited by an intensity level curve through the *delimiting saddle point* P_{saddle} of the grey level blob.

For bright blobs, the extremum point is a local maximum and the delimiting saddle point is the highest possible point, where a path can be traced to both the local maximum belonging to the blob, and another local maximum, without descending below the saddle point. The *support region* G_R of the blob is the set of points inside the delimiting level curve, that have an intensity value greater than the intensity of the level curve (see figure 1).

The volume $G_{vol-rel}$ of the grey-level blob at scale t with original relative base level is defined as

$$G_{vol-rel} = \int_{G_R} L(x,t) - L(P_{saddle},t)\, dx \tag{10}$$

Later, this entity will be used when formulating a quantitative measure of the significance of the grey-level blob.
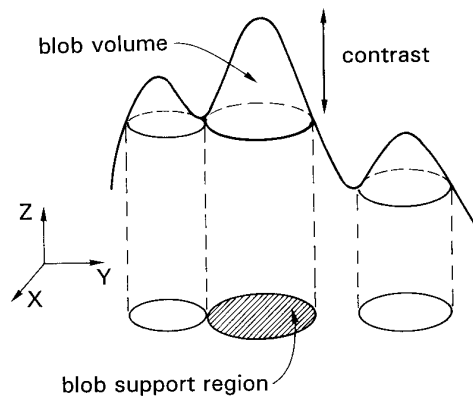

Figure 1: Definition of the grey-level blob in the two-dimensional case. The intensity is along the Z-axis.

2.3.2 Grey-level blobs with absolute base level

An alternative approach for measuring the grey-level blob volume is to use an absolute base level. The motivation for the relative base level is that in intensity images there is no absolute reference level to relate the intensity measurements to. When analyzing data with an absolute reference level, such as those produced by the general linear model, one may consider the approach of defining the grey-level blob volume relative to this reference level. Thus, the grey-level blob volume with absolute base-level is defined by

$$G_{vol-abs} = \begin{cases} \int_{G_R} L(x,t)\,dx & if\ L(P_{saddle},t) \geq 0 \\ \int_{G_R} L(x,t) - L(P_{saddle},t)\,dx & if\ L(P_{saddle},t) < 0 \end{cases} \tag{11}$$

where G_R is the support region and P_{saddle} is the position of the delimiting saddle point for this grey-level blob. This relates the blob volumes to the absolute zero base level suitable for PET images. To have a graceful transition for blobs with a negative saddle point intensity, the calculation of the volumes for these blobs uses the intensity of the saddle point as the base-level. This definition is illustrated in figure 2.
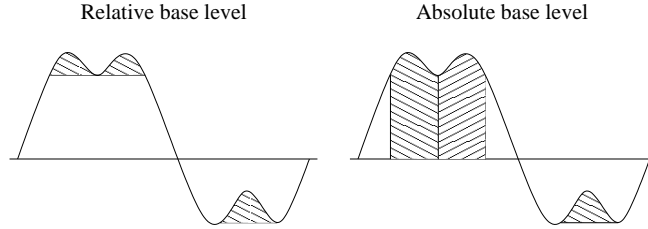

Figure 2: The definition of grey-level blob volume using a relative base level is based on local contrasts measured relative to the delimiting saddle point of the grey-level blob, while definition of grey-level blob volume using absolute base level is based on contrasts relative to a zero base level. For blobs that contain negative intensity values, however, we always use the definition in term of relative base level.

2.3.3 Scale-space blobs

The grey-level blobs are detected at every scale in the scale-space representation. By tracking the extremum points of grey-level blobs in the scale direction, grey-level blobs can be grouped together to form scale-space blobs. These scale-space blobs are delimited in the scale direction by bifurcation events, which represent changes in the structure of the extremum points and therefore qualitative changes between grey-level blobs. The four possible bifurcation events are, blob merge, blob split, blob creation and blob annihilation (see figure 3). These bifurcations link the different scale-space blobs together into a hierarchical structure.

Some useful properties of the scale-space blobs can be defined. First we define the *most significant grey-level blob* of the scale-space blob as the grey-level blob with the maximum effective volume as measured by equation (12) within the scale-space blob. The *support region* of the scale-space blob (S_R) is then defined as the support region of the most significant grey-level blob and the *selected scale* is defined as the scale of the most significant grey-level blob.

The lowest scale where the scale-space blob first appears is denounced as the *appearance scale* (t_{appear}) of the scale-space blob and the scale where the scale-space blob disappears is denounced the *disappearance scale* ($t_{disappear}$).
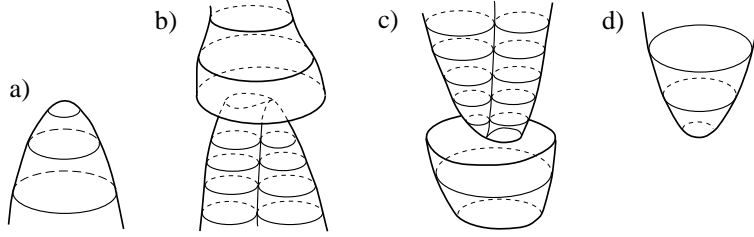
Figure 3: Generic blob events in the scale-space (a) annihilation, (b) merge, (c) split, (d) creation. Here, the scale parameter is along the vertical axis.

2.3.4 Significance of scale-space blobs

The significance measure of the scale-space blobs should be a measure of the underlying structure of the activations in the image. A more significant activation should result in a higher significance measure and noise should give scale-space blobs with lower significance measures. As argued in (Lindeberg, 1993), the following following components are natural to include in a significance measure:

- spatial extent x: A grey-level blob having large spatial extent, may be treated as more significant than a smaller grey-level blob.

- contrast z: A grey-level blob with a high contrast value may be treated as more significant than a similar grey-level blob with a lower contrast.

- lifetime τ: A grey-level blob with a long lifetime in scale-space, may be treated as more significant than a similar grey-level blob with a shorter lifetime.

Measuring spatial extent and contrast.   When measuring spatial extent and contrast, a natural requirement is to allow for comparison of grey-level blob volumes across scales. This is done by normalizing the grey-level blob volume G_{vol} by

$$V_{prel} = \frac{G_{vol} - V_m(t)}{V_\sigma(t)} \tag{12}$$

where $V_m(t)$ is the mean and $V_\sigma(t)$ the standard deviation of grey-level blob volumes at the scale t. The $V_m(t)$ and $V_\sigma(t)$ functions are estimated from statistics reference noise images. (see section 3.1)

The entity V_{prel} is, however, not suitable for scale integration, since it can assume negative values. A normalization that empirically has given reasonable results is

$$V_{eff} = \begin{cases} 1 + V_{prel} & when \ V_{prel} \geq 0, \\ e^{V_{prel}} & when \ V_{prel} < 0. \end{cases} \tag{13}$$

Measuring scale lifetime.   When measuring scale lifetime it is natural to require that the expected lifetime of a scale space blob should not vary over scales. This leads to a transformation function of the form

$$\tau_{eff}(t) = C_1 + C_2 \log(p(t)) \tag{14}$$

where $p(t)$ is the expected density of extrema at scale t and C_1 and C_2 are constants, where C_1 without loss of generality can be set to zero. In our case, $\tau_{eff}(t)$ is calculated as

$$\tau_{eff}(t) = \log\left(\frac{p_{ref}(0)}{p_{ref}(t)}\right) \tag{15}$$

where $p_{ref}(t)$ denotes the average density of local extrema as a function of scale t.

Computing the scale space volume. Finally, given the transformed entities τ_{eff} and V_{eff}, the scale-space blob volume is then defined by

$$S_{vol} = \int_{t_{appear}}^{t_{disappear}} V_{eff}(t) d\tau_{eff}(t) \qquad (16)$$

where t_{appear} is the appearance scale of the scale-space blob, $t_{disappear}$ is the disappearance scale of the scale-space blob. The entity S_{vol} will be used as the significance measure for the scale-space blob, and thus for ranking brain activations in order of significance.

3 Methods

3.1 Collecting reference statistics

The definition of the scale-space blob volume according to (16) as a significance measure for ranking blobs in order of significance relies on the the accumulation of reference statistics of the behavior of blob descriptors in scale-space, in order to allow for the comparison between image structures at different scales. The idea is that reference statistics of $V_m(t)$, $V_\sigma(t)$ and $p_{ref}(t)$ in (12) and (15) should be collected for representative image data containing noise with similar characteristics at the PET images, however, disregarding the effect of coarser scale brain activations.

In the original work on the scale-space primal sketch for computer vision applications, white noise was used for this normalization purpose. The idea behind this choice was to estimate to what extent accidental groupings occur in scale-space (Lindeberg, 1993). Later, also self-similar noise patterns have been considered for scale normalization (Lindeberg, 1998). When analyzing PET images, however, the imaging and reconstruction procedures lead to a preferred inner scale of the data, which we want to capture in order to avoid an unnecessary bias to image structures corresponding to these artifacts related to the imaging procedure. For these reasons, difference images between different PET experiments as well as student-t images from PET experiments were used for scale normalization (Lindeberg et al., 1999).

In this work, we will use an extension of these ideas, by taking the detailed structure of the pre-processing stages to the scale-space analysis into account. We propose that the residual noise images $\varepsilon(x)$ obtained from the general linear model (1) are ideally suited for the collection of reference statistics for scale normalization. The idea behind this choice is that the general linear model applied to the composed PET experiment should capture the overall brain activations in the data, and that image structures that are not captured by this model could be regarded as a reasonable estimate of the noise characteristics. Preliminary results by (Björkman et al., 1999) demonstrate that this model has attractive properties for separating blobs representing brain activations in PET images from blobs extracted from noise patterns.

Figure 4 shows reference statistics of $V_m(t)$, $V_\sigma(t)$ collected in this way for 30 images, using relative base level as well as absolute base level. For comparison, corresponding results of using white noise normalization are also shown.

3.2 Merging of multiple responses

When using the scale-space primal sketch in practice, it sometimes occurs that an activation in the image is represented by multiple blobs in the scale-space primal sketch, although we from an intuitive viewpoint would regard the these blobs as corresponding to the same image structure. (For one example, see figure 5 on page 12.)
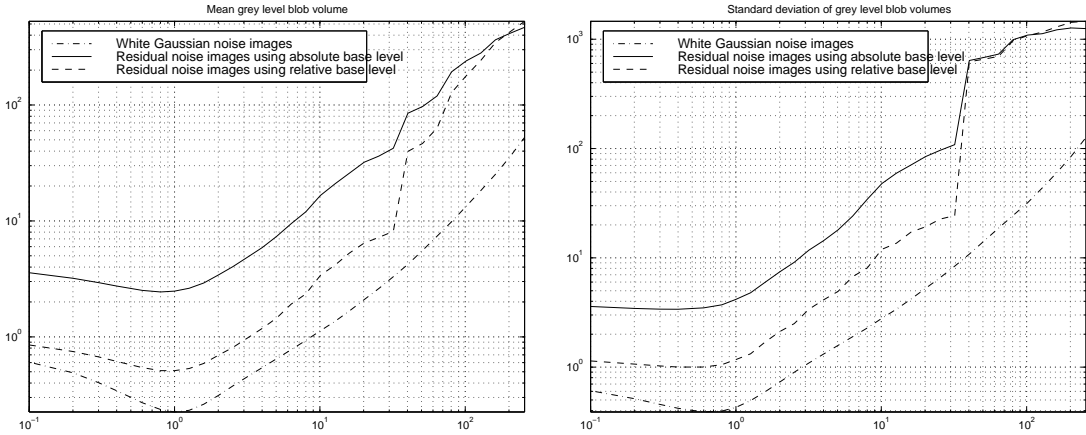
(a) The mean of grey level blob volumes for different noise images.

(b) The standard deviation of grey level blob volumes for different noise images.

Figure 4: Reference statistics of V_m and V_σ collected for 30 residual noise images, using absolute vs. relative base level, as well as corresponding reference statistics for 100 white noise images.

The reason why this occurs is usually that a large (significant) blob merges with a smaller (insignificant) blob and forms a new scale-space blob. This will result in lower significance in each of the blobs than the activation would otherwise give. To reduce the influence of such effects, we will in this section present an algorithm for merging multiple blob responses. This post-processing step substantially simplifies the interpretation of the output from the scale-space primal sketch.

Next, we will propose a number of conditions to indicate when two blobs should be merged. The criteria to be fulfilled are the following:

3.2.1 Qualitative criteria for merging overlapping scale-space blobs

The basic idea of the merge algorithm is to regard two scale-space blobs b_A and b_B as candidates for a blob merge if their support regions largely overlap. We require that the extremum point P_e of scale-space blob b_A is included in the support-region S_R of the other blob b_B and vice versa, formalized as:

$$mergecand(b_A, b_B) = \begin{array}{l} (P_e(b_A) \in S_R(b_B)) \wedge \\ (P_e(b_B) \in S_R(b_A)) \end{array} \quad (17)$$

3.2.2 Quantitative criteria for merging scale-space blobs

In addition to the previous qualitative criterion, it is useful to define a number of quantitative measures. These will make it less likely that two scale-space blobs are merged if they represent different activations.

Proximity in scale. Consider two scale-space blobs b_A and b_B, where b_A exists at coarser scales than b_B. Then, a merge is accepted only if

$$\frac{t_{appear}(b_A)}{t_{disappear}(b_B)} < s_{treshold} \quad (18)$$

Similarity in the size of the support region. A merge between two scale-space blobs b_A and b_B is accepted only if the size of the support region is similar. That is, if

$$\left| \log \frac{size[S_R(b_A)]}{size[S_R(b_B)]} \right| < v_{treshold} \tag{19}$$

3.2.3 Merging order

Two scale-space blobs b_A and b_B are considered for a merge only if all the previous conditions are satisfied. After establishing that two blobs could be merged, one has to establish in which order the merging should occur. In this application, we first group all blobs that are related according to the abovementioned criteria into groups. Then, within each group, we first merge the two blobs that are nearest to each other in the scale direction.

Here, distances in the scale direction are measured as relative variations. For two scale-space blobs b_A and b_B, where b_A exists at coarser scales than b_B, the distance $d(A, B)$ between these blobs is defined as

$$d(b_A, b_B) = d_{AB} = \log \frac{t_{appear}(b_A)}{t_{disappear}(b_B)} \tag{20}$$

3.3 Merging of blobs

When merging two scale-space blobs, there are two natural ways to compute the significance value of the new blob. One approach is to just add the scale-space blob volumes of the scale-space blobs. This is clearly a conservative approach. Another approach is to extend the extent of the scale-space blob over the entire scale range of the two primitive scale-space blobs, and to fill in the scale interval in between. The significance value of the merged scale-space blob will then be composed of both the sum of the two primitive scale-space blob volumes, incremented by the result of interpolating grey-level blob volumes in the scale interval in between. Here, the latter approach is chosen.

3.4 Composed scale-space blob merging algorithm

In summary, the blob merging algorithm consist of the following steps. Let the set of all scale-space blobs in the image be denoted by B. Each blob in B is denoted by b_i, where $1 \leq i \leq n$ and n is the number of blobs. If the conditions (17), (18) and (19) in sections 3.2.1 and 3.2.2 are satisfied, then we say that the *blob merge criterion* $C(b_i, b_j) = c_{ij}$ is true. Since this relationship is symmetric, it follows that $c_{ij} = c_{ji}$.

1. For each blob b_i, select the subset $M(b_i)$ that consist of all blobs b_j that satisfy $c_{ij} = true$.

2. All blobs with empty subsets $M(b_i)$ are moved to a set F. These blobs do not need further processing.

3. Within each subset $M(b_i)$, compute the distances d_{ij} in the scale direction according to equation (20) between all pairs (b_i, b_j) of blobs in this subset.

4. For each subset $M(b_i)$, determine the blob $b_{\min}(b_i)$ with the minimum distance $d_{\min}(b_i)$ where

$$d_{\min}(b_i) = \min_{\{j : c_{ij} = true\}} d(b_i, b_j) \tag{21}$$

5. If a pair of blobs (b_j, b_k) satisfies $(b_{\min}(b_j) = b_k) \wedge (b_{\min}(b_k) = b_j)$, then these blobs are merged to a new blob b_l. All relevant descriptors for b_l are computed. All blobs in the subsets $M(b_j)$ and $M(b_k)$ are tested according to the blob merge criteria against b_l and possibly included in subset $M(b_l)$. Finally, the blobs b_j and b_k are removed.

6. Continue with step 2-5 until there is no non-empty subset $M(b_i)$.

3.5 Parameter setting of merging algorithm

There are two free parameters in the algorithm, $s_{treshold}$ in equation (18) and $v_{treshold}$ in equation (19):

- $v_{treshold}$ is a threshold determining when two scale-space blobs are sufficiently similar in size. Here, we use $\log 2^D$, where D is the dimensionality of the data.

- $s_{treshold}$ is a threshold determining when two blobs are sufficiently close enough in scale direction. Here, we use $s_{treshold} = 2^2$.

These parameter settings have been demonstrated to give reasonable results in our experiments, and are kept constant.

3.6 Measure of significance change

To quantify how much the significance values are affected by measuring the grey-level blob volumes using an absolute base level compared to a relative base-level, we introduce a measure of significance change in the following way:

First, a regression model is computed between the scale-space blob volumes $S_{vol-rel_i}$ using relative base level and the scale-space blob volumes $S_{vol-abs_i}$ using absolute base level. In other words, a constant c is fitted from a least squares fit of

$$\log_{10} S_{vol-abs_i} = \log_{10} S_{vol-rel_i} + \log_{10} c \tag{22}$$

over a range of blobs, where we have introduced a logarithmic transformation to emphasize the impact of relative variations. Then, a local descriptor D_i of how much the significance value has changed for a single blob is defined as

$$D_i = \log_{10} S_{vol-abs_i} - \log_{10} S_{vol-rel_i} - \log_{10} c \tag{23}$$

This local descriptor gives us an indication of how much the significance have changed in comparison to other blobs in the same image when changing the significance measure.
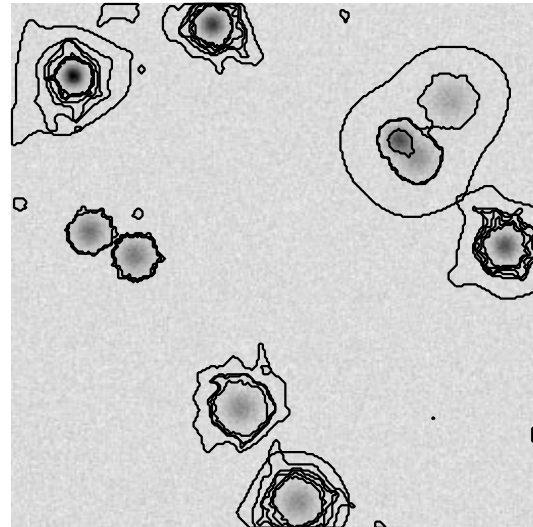
4 Experiments

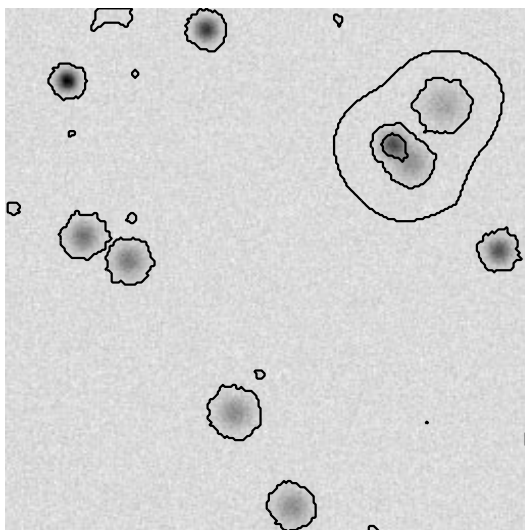## 4.1 Blob merging on synthetic images with noise

To evaluate the behavior of the merging algorithm, we shall first investigate its behavior on synthetic images consisting of randomly positioned Gaussian peaks with added white Gaussian noise.
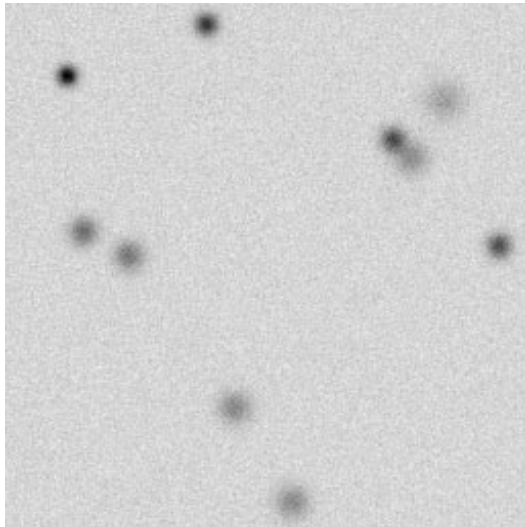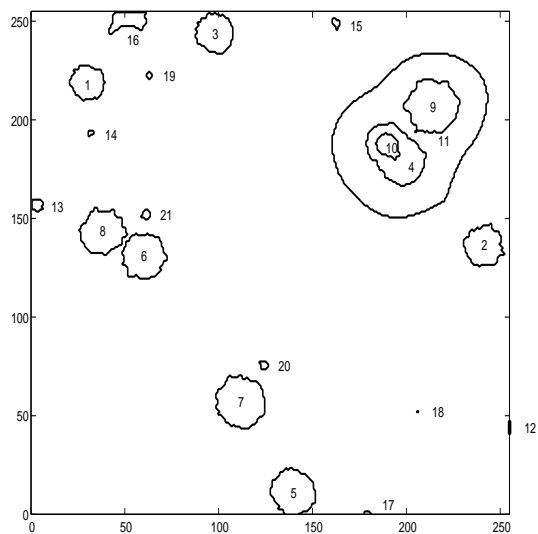
(a) Original image with 10 Gaussian peaks and white Gaussian noise.

(b) The 50 most significant scale-space blobs, detected from the grey-level image

(c) Blob support regions after merging.

(d) Ranking of the blobs after merging, overlayed on blob boundaries.

Figure 5: The result of applying the blob merging algorithm to a synthetic image with 10 Gaussian peaks and added white Gaussian noise. We can see that the number of blob responses has been reduced significantly. Besides accidental groupings of nearby peaks, there is one blob response for each Gaussian peak.

Experimental setup.   Ten Gaussian peaks, all with the same integral mass of 20, and randomly selected standard deviations σ in $[3, 10]$ were randomly positioned in a 256x256 image. White Gaussian noise with standard deviation of 0.01 was added to the signal (figure 5(a)). The noise level was selected to induce the effect of high blob fragmentation. The scale-space primal sketch was applied to this image, and the 50 most significant blobs were selected (figure 5(b)). Originally there were about 10^4 scale-space blobs in the data.

Evaluation of blob merging.   As can be seen from the results in figure 5(b), some of the Gaussian peaks give rise to multiple blob responses. Figure 5(c) shows the results after blob merging, using the algorithm in section 3.4. As can be seen, the results are intuitively very reasonable. For most of the Gaussian peaks, there is a unique corresponding scale-space blob and this blob has a high significance value. For three nearby blobs in the upper right corner, the algorithm in addition finds blobs corresponding to the union of two or more nearby blobs. These blobs correspond to hierarchical grouping of the blobs, and should not be merged by the algorithm.

Evaluation of the significance value.   The significance value gives a quantitative measure of the relative strength of the signals. A higher significance value should reflect a lower likelihood that a blob was created by random noise. Table 1 and 2 show the fifteen most significant scale-space blobs, before and after merging. The total number of blobs was limited to 50 before merging to simplify analysis. The D_i column gives a measure of how much the relative significance of the blob has changed (see section 3.6). It can be seen that the significance value has changed significantly for some blobs. For example, the blobs ranked as number 1, 2 and 3 after merging were previously ranked as number 5, 6 and 7 respectively and the significance value has increased by a factor of at least 4 for these blobs.

When comparing the tables with the images, it is clear that the new ranking corresponds well with what would have been expected. The 10 most significant blobs

rank	significance	scale	extremum point (x, y)
1	49.85	2.19	(189, 189)
2	37.11	1.10	(60, 132)
3	35.78	1.17	(38, 144)
4	25.56	1.61	(216, 207)
5	19.76	1.70	(30, 220)
6	18.27	1.97	(241, 137)
7	15.32	1.46	(98, 245)
8	13.81	11.85	(112, 58)
9	13.45	2.99	(98, 245)
10	13.40	0.75	(98, 245)
11	11.39	2.54	(140, 12)
12	11.18	1.10	(30, 220)
13	10.31	1.38	(112, 58)
14	9.82	10.43	(140, 12)
15	9.78	0.61	(241, 137)

Table 1: The 15 most significant blobs in the image before merging multiple responses on the synthetic image in figure 5. The scale column represents the scale of the most significant grey-level blob in the scale-space blob. By comparison with table 2 one can see that the blob ranking is heavily affected by the blob merging algorithm.

rank	significance	scale	extremum point (x, y)	blobs before merge	D_i
1	71.03	0.61	(30, 220)	5, 12, 17, 21, 27, 29, 36, 39	0.4064
2	65.32	0.61	(241, 137)	6, 15, 22, 25, 26, 33	0.4040
3	64.52	0.75	(98, 245)	7, 9, 10, 18, 32, 50	0.4751
4	59.51	1.70	(189, 189)	1, 16	-0.0724
5	50.37	1.03	(140, 13)	11, 14, 19, 20, 35, 38	0.4963
6	47.65	0.89	(59, 132)	2, 28, 49	-0.0408
7	44.92	1.38	(112, 58)	8, 13, 23, 30	0.3631
8	40.91	1.17	(38, 144)	3, 34	-0.0911
9	25.56	1.61	(216, 207)	4	-0.1493
10	6.10	0.54	(189, 189)	24	-0.1493
11	4.87	108.64	(193, 186)	31	-0.1493
12	4.07	31.38	(255, 45)	37	-0.1493
13	3.90	1.31	(4, 159)	40	-0.1493
14	3.75	1.61	(32, 195)	41	-0.1493
15	3.63	1.17	(162, 251)	42	-0.1493

Table 2: The 15 most significant blobs after merging of multiple responses. It is clear that the merged blobs in general have a higher ranking than previously. The unaffected blobs have kept their significance value, while their *relative* significance with respect to other blobs have decreased as measured by the D_i value.

correspond to the ten Gaussian peaks. Blob number 11 represents the merging of two Gaussian peaks and the other blobs are due to noise. There is a large difference in the level of significance between the blobs representing signal and blobs representing noise and a high correspondence between strength of the underlying signal and the significance measure. There is a clear cut in the significance between blob number 9 and 10 with blobs above representing signals and blobs below responding mainly to noise. The exceptions is blob number 10, which is heavily affected by its nearby neighbors, and number 11, which represent a hierarchical grouping of several blobs at a coarse scale.

It can also be observed that blobs with high significance correspond to Gaussian peaks with a narrow width and high intensity. This is consistent with our expectation, since high amplitude blobs are less likely to originate from random phenomena.

Test of ten images. Similar experiments were done for 10 other random Gaussian blob images. As a whole, these experiments support our previous conclusions. One minor exception was noted, where in one case the algorithm merged two scale-space blobs in a situation where a merge bifurcation should have been kept.

4.2 Experiments on 2-D PET images

Next, we turn to real PET data. Initially, we consider two-dimensional slices which are easiest to visualize.

Experimental setup. Five sagittal slices were extracted from a contrast image, derived from a tactile visual experiment (described in more detail in section 4.3) and prefiltered with 5 mm full width half maximum Gaussian filter. The statistics used by the subsequent scale-space primal sketch calculation was generated from these five slices.

Figure 6(a) shows a sagittal slice from the contrast. Figure 6(b) shows the 100 most significant scale-space blobs extracted from this two-dimensional data set using relative

Index_abs	Sign_abs	Scale_abs	Index_rel	Sign_rel	Scale_rel	D_i
1	15.53	8.43	1	14.24	8.43	-0.0112
2	14.44	1.32	12	3.11	1.32	0.6186
3	10.21	0.00	10	3.61	0.00	0.4029
4	6.73	0.00	4	5.64	0.00	0.0277
5	5.79	0.00	3	7.75	0.00	-0.1751
6	5.34	0.00	17	2.18	0.00	0.3412
7	5.22	0.28	2	8.15	0.28	-0.2420
8	4.31	7.11	7	5.05	7.11	-0.1173
9	4.02	0.00	8	4.42	0.65	-0.0905
10	3.76	0.17	6	5.21	0.17	-0.1904
11	3.68	0.00	5	5.60	0.00	-0.2310
12	2.97	0.00	18	2.16	0.00	0.0886
13	2.97	0.00	9	3.65	0.00	-0.1391
14	2.54	0.17	16	2.31	0.17	-0.0082
15	2.52	0.65	14	2.67	0.65	-0.0741
16	2.48	0.28	20	1.72	0.28	0.1094
17	2.39	0.00	13	2.82	0.00	-0.1217
18	2.38	0.00	11	3.40	0.00	-0.2042
19	2.27	0.00	15	2.37	0.00	-0.0667
20	2.17	0.00	21	1.60	0.00	0.0829

Table 3: Table of significance values for the blobs in figure 6. Index_abs represent calculation with absolute base level and Index_rel relative base level. D_i is calculated according to section 3.6. A positive D_i value indicates greater significance for the absolute base level blob. From the D_i values, it can be seen that blobs #2 and #3 have been assigned a substantially higher significance value when using absolute base level compared to relative base level. As can be seen from figure 6(f), these blobs are substructures of a coarse scale blob.

base level. Figure 6(c) shows the scale-space blobs after merging of multiple responses and figure 6(d) corresponding results using absolute instead of relative base level.

By comparing figure 6(b) and figure 6(c) we can observe that a substantial reduction of multiple blob responses is obtained by the blob merging algorithm.

Specifically, most of the candidates for merging, which intuitively should be merged, have been merged with a few exceptions. Thus, the blob merging algorithm appears suitable for its intended purpose.

Absolute versus relative base level of the scale-space blobs. A comparison between the results of blob extraction using relative base level in figure 6(c)(e) and absolute base level in 6(d)(f) was performed. The corresponding significance measures can be found in table 3. The images and table reveal the following properties:

The size, shape and position of the blobs remain essentially the same in these two cases. The significance value and relative ranking of the blobs is, however, substantially affected for certain blobs. Typically, the significance value for blobs that are substructures of large blobs are much greater when using absolute base level than relative base level. Notice especially blob number 10 and 12 calculated with relative base level, which when using absolute base level have changed to ranking number 3 and 2 respectively. For isolated blobs, on the other hand, the significance values are essentially the same.
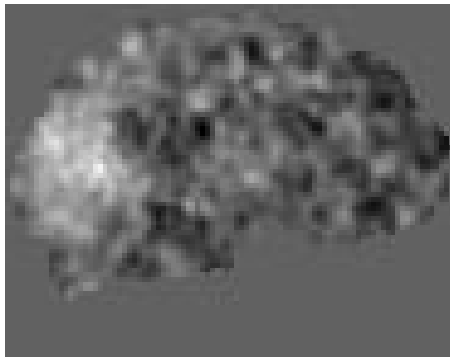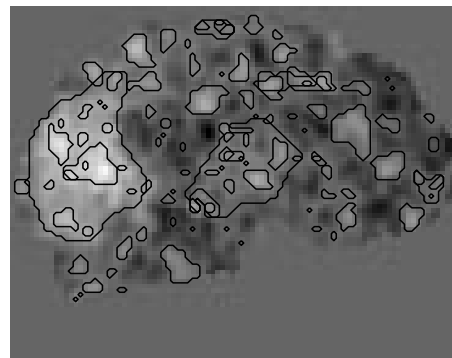
(a) The original data to be analyzed. A sagittal slice from the visual-tactile experiment, prefiltered with 5mm FWHM Gaussian filter.
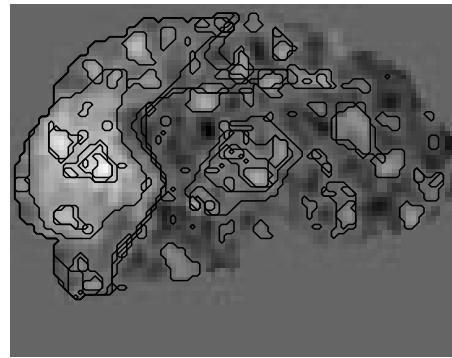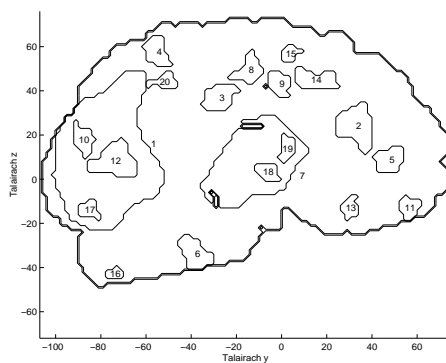
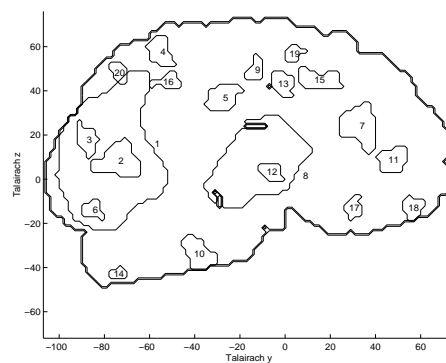(b) The 100 most significant blobs found by a 2-D scale-space primal sketch analysis.
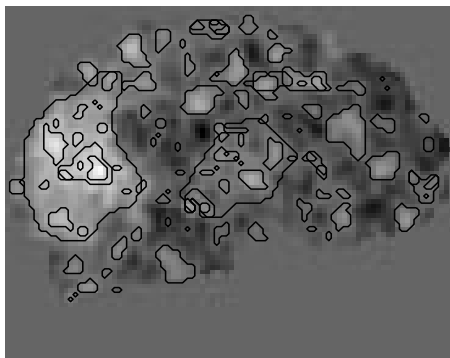
(c) Blobs left after merging of multiple responses, here using relative base level.

(d) Blobs left after merging of multiple responses, here using absolute base level.

(e) The 20 most significant blob rankings after merging of multiple responses, using relative base level.

(f) The 20 most significant blob rankings after merging of multiple responses, using absolute base level.

Figure 6: Comparison between absolute and relative base-level for a 2-D sagittal slice of a PET image, from a visual-tactile discrimination test. From the comparison of blob rankings in the bottom row, it can be seen that substructures in the large blob corresponding to the visual areas are assigned a much higher significance when using absolute base level compared to relative base level. (See table 3)

4.3   Experiments on 3-D PET images

A study has been performed to evaluate the effect of using absolute base level instead of relative base level on real 3-D PET data. Two different PET experiments were used for this evaluation. One study involved a tactile-visual contrast where the subject had an ellipsoid in their hand and was supposed to match it to visually presented ellipsoids of different shapes. The second study was a forced choice discrimination test, where the subject was to choose which one of two parallellepipeda had the most oblong shape.

Tactile visual experiment.   This study, originally described in (Hadjikhani and Roland, 1998), consists of eight test subjects, performing four different test conditions with three repetitions of every test condition. Some PET-images were excluded due to artifacts and the total number of images used in the study was 93. The test conditions consisted of matching between different ellipsoids, presented visually and tactically, to the subjects. The four test-conditions were, tactile-tactile matching (TT), tactile-visual matching (TV), visual-visual matching (VV) and a motor control resting condition (rest).

The PET images were realigned within subjects to compensate for movements between acquisitions, and reformatted to standard form using the human brain atlas of (Roland et al., 1994). There was no prefiltering of the data at this stage. These preprocessed images formed the input data to the general linear model, described in section 2.1. Thirteen parameters were used in the model: one for the mean, four for the different test-conditions and eight for the test subjects.

The residual noise $\varepsilon_i(x)$ in the general linear model was used for estimating the noise in the PET-images. From the $\varepsilon_i(x)$ images, a number of synthetic random noise images were derived through a process described in (Ledberg, 1999). The synthetic random noise images were used to estimate $V_m(t)$, $V_\sigma(t)$ and $\tau_{eff}(t)$ in the scale-space primal sketch.

The contrast derived from the GLM model was the tactile-visual contrast with all the subjects and repetitions in it. This is the same contrast as in (Lindeberg et al., 1999). The contrast image was analyzed in 3-D with the scale-space primal sketch. Multiple responses were merged and a mask was applied to remove scale-space blobs outside the brain.

Results.   The result of the analysis with absolute base level can be seen in figure 7 and in table 4. Corresponding results using relative base level are presented in figure 8 and table 5. When using absolute base level we can see that the most significant blobs tend to appear in the region of the brain near the visual cortex, while when using relative base level, the most significant blobs are more evenly spread throughout the brain. This is consistent with our expectations, since the visual cortex as a whole is more activated than the rest of the brain in this experiment. This will make the small activated regions, like number 1 and 4 when using absolute base level, that are superimposed on the visual cortex to gain the most in significance by changing the base level to zero. Other blobs, like number 5 which is located far from any neighbors, have the same ranking in both figures.

The blobs have been compared to the significant regions found in (Hadjikhani and Roland, 1998) using the analysis method suggested by (Roland et al., 1993) to measure the statistical significance. As can be seen in the tables, nine of the blobs were also regarded as significant by (Hadjikhani and Roland, 1998). When comparing the relative base level blobs, five were regarded as significant in (Hadjikhani and Roland, 1998).
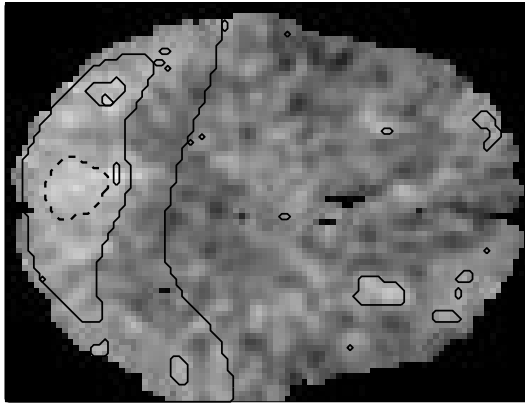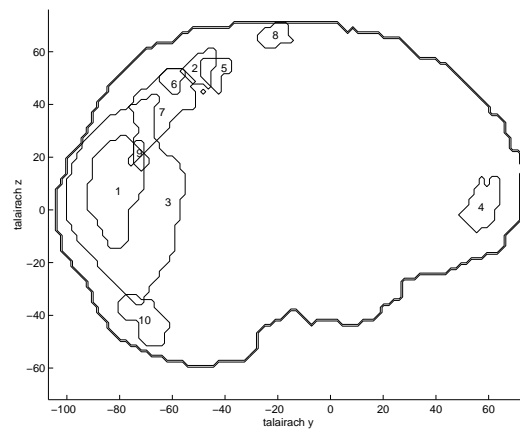
(a) Horizontal slice (z=8) of the contrast image with superimposed blobs. The image is visualized filtered with a 5mm full width half maximum Gaussian filter. In the analysis, non-filtered data are used.
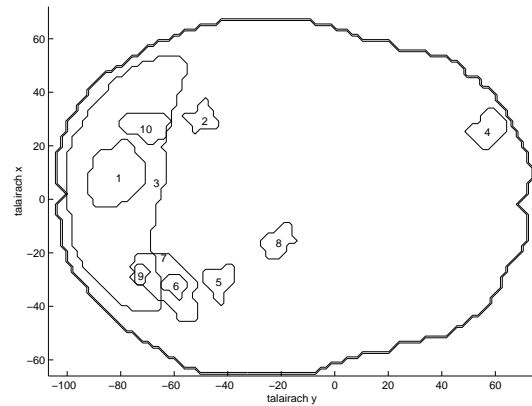
(b) Outline of the ten most significant blobs in the horizontal plane, viewed from above.
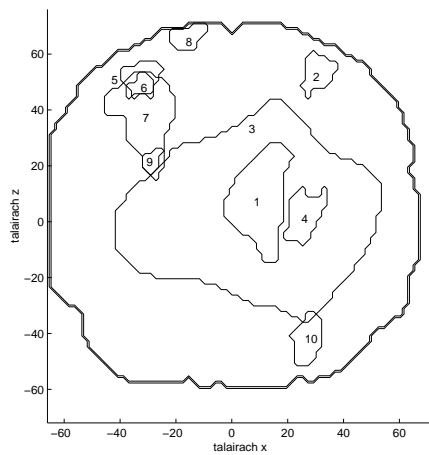
(c) Outline of the ten most significant scale-space blobs in the coronal plane, viewed from the front.

(d) Outline of the ten most significant scale-space blobs in the sagittal plane, viewed from the subjects right side.

Figure 7: The ten most significant blobs from visual-tactile experiment, analyzed by the 3-D scale-space primal sketch using *absolute* base level, here shown in sagittal, coronal and horizontal cuts. Note (from a comparison with figure 8) that when using absolute base level, the superimposed blobs located in the rear part are assigned a higher significance.

(a) Horizontal slice (z=8) of the contrast image with superimposed blobs. The image is visualized filtered with a 5mm full width half maximum Gaussian filter. In the analysis, non-filtered data are used.

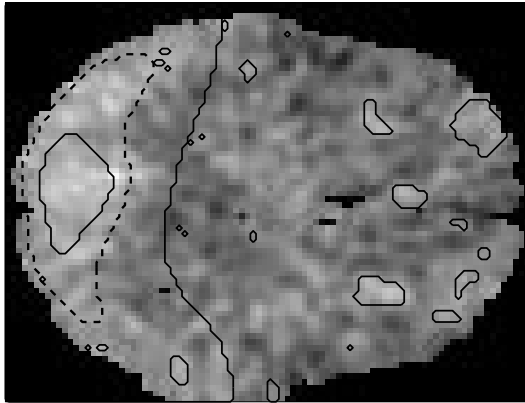(b) Outline of the ten most significant blobs in the horizontal plane, viewed from above.

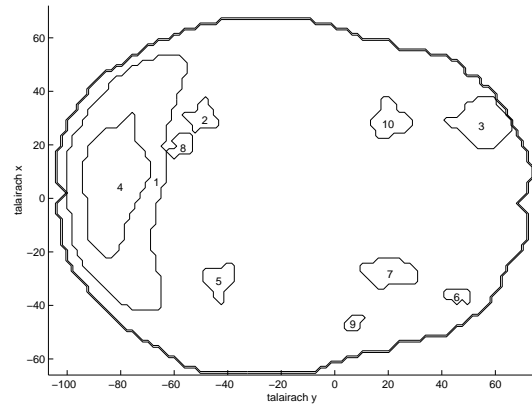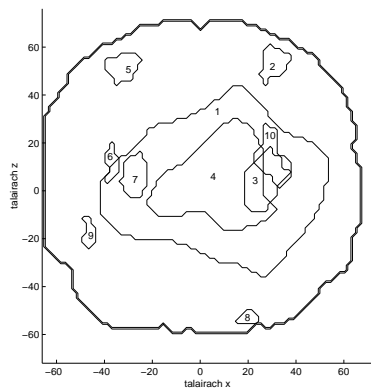(c) Outline of the ten most significant scale-space blobs in the coronal plane, viewed from the front.
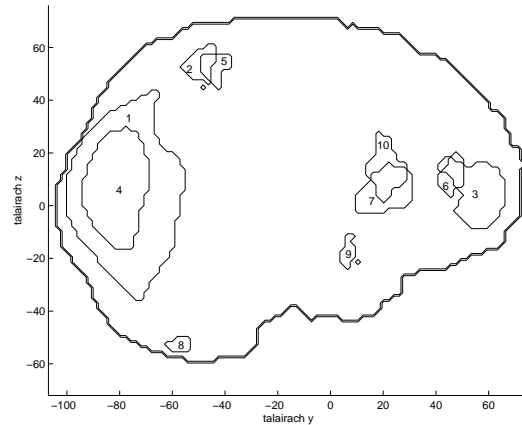
(d) Outline of the ten most significant scale-space blobs in the sagittal plane, viewed from the subjects right side.

Figure 8: The ten most significant blobs from visual-tactile experiment, analyzed by 3D scale-space primal sketch with *relative* base level, here shown in sagittal, coronal and horizontal cuts.

| Index abs	Sign	Scale	Position	Vol mm³	Prev. sig	Index rel	Sign rel	D_i	Region name
1	71.67	5.92	(8, -82, 8)	8672	yes	4	31.99	0.1170	visual cortex (V1,V2)
2	69.89	0.80	(34, -48, 54)	736	yes	2	58.28	-0.1544	somatosensory association cortex
3	59.89	20.57	(10, -82, 8)	114704	yes	1	70.98	-0.3071	visual cortex
4	47.67	1.65	(26, 57, -1)	1392	yes	34	10.19	0.4366	sulcus frontalis sup. sin.
5	39.32	1.25	(-31, -44, 54)	776	yes	5	24.65	-0.0307	lobus pareitalis sup. dxt.
6	28.55	0.86	(-33, -62, -52)	336	yes	12	15.10	0.0434	lobus pareitalis sup. post. dxt.
7	27.58	6.36	(-31, -60, 46)	5816	yes	23	12.37	0.1147	sulcus intraparetalis dxt.
8	25.25	1.51	(-19, -22, 68)	656	yes	25	12.21	0.0824	premotor cortex dxt.
9	24.35	0.42	(-27, -72, 20)	248	yes	14	14.74	-0.0152	visual cortex lobus occipitalis
10	21.91	2.31	(28, -70, -41)	1496	no	21	12.59	0.0073	lobus post. sin. cerebellum
11	21.82	0.70	(22, -56, -53)	256	no	8	16.91	-0.1224	lobus post. dxt.
12	21.69	2.94	(4, -58, 54)	1936	yes	13	14.76	-0.0661	precuneus sin.
13	19.42	2.49	(-13, -88, 1)	1048	yes	93	6.43	0.2465	visual cortex (V1, V2)
14	18.94	0.19	(34, -62, 52)	168	yes	24	12.34	-0.0473	sulcus intrapareitalis sin.
15	18.69	0.59	(54, -54, 12)	368	no	33	10.26	0.0274	gyrus temp. sup. sin.

Table 4: Table of the ten most significant blobs analyzed with *absolute* base level. The columns are; (Index abs) blob ranking, (Sign) scale-space significance, (Scale) scale of the scale-space blob, (Position) position in Talairach coordinates, (Vol) volume of the scale-space blob support region, (Prev. Sig) if the blob was previously regarded as significant according to (Hadjikhani and Roland, 1998), (Index rel) index of corresponding relative blob, (Sign rel) significance of corresponding relative blob, (D_i) measure of the change of significance according to section 3.6 and (Region name) name of activated region. The location and shape of the blobs can be viewed in figure 7.

| Index rel	Sign	Scale	Position	Vol mm³	Prev. sig	Index abs	Sign abs	D_i	Region name
1	70.98	20.58	(10, -82, 8)	114704	yes	3	59.89	0.0941	visual cortex
2	58.28	0.80	(34, -48, 54)	736	yes	2	69.89	-0.0586	somatosensory association cortex
3	53.44	2.94	(26, 59, -1)	4120	yes	4	47.67	0.0699	sulcus frontalis sup. sin.
4	31.99	12.14	(10, -82, 10)	22120	yes	1	71.67	-0.3301	visual cortex (V1, V2)
5	24.66	1.25	(-31, -44, 54)	776	yes	5	39.32	-0.1823	lobus pareitalis sup. dxt.
6	23.15	0.43	(-37, 49, 12)	392	no	25	14.26	0.2307	sulcus frontalis sup. dxt.
7	17.36	2.31	(-29, 19, 4)	2072	no	22	15.63	0.0659	insula anterior dxt.
8	16.91	0.70	(22, -56, -53)	256	no	11	21.82	-0.0906	lobus posterior sin. cerebellum
9	16.27	0.37	(-47, 7, -19)	184	no	68	8.29	0.3132	polus temporalis dxt.
10	15.99	2.94	(30, 21, 14)	1560	no	61	9.03	0.2687	insula anterior sin.
11	15.29	0.86	(34, -15, -15)	424	no	44	10.44	0.1860	amygdala sin.
12	15.10	0.86	(-33, -62, 52)	336	yes	6	28.55	-0.2565	lobus pareitalis sup. post. dxt.
13	14.76	2.94	(4, -58, 54)	1936	yes	12	21.69	-0.1469	precuneus sin.
14	14.74	0.43	(-27, -72, 20)	248	yes	9	24.35	-0.1979	visual cortex lobus occipitalis
15	14.45	0.19	(-43, -5, -33)	80	no	69	8.23	0.2527	polus temporalis dxt.

Table 5: Table of the ten most significant blobs analyzed with *relative* base level. The columns are; (Index rel) blob ranking, (Sign) scale-space significance, (Scale) scale of the scale-space blob, (Position) position in Talairach coordinates, (Vol) volume of the scale-space blob support region, (Prev. sig) if the blob was previously regarded as significant according to (Hadjikhani and Roland, 1998), (Index abs) index of corresponding absolute blob, (Sign abs) index of corresponding absolute blob, (D_i) measure of the change of significance according to section 3.6 and (Region name) name of activated region. The location and shape of the blobs can be viewed in figure 8.
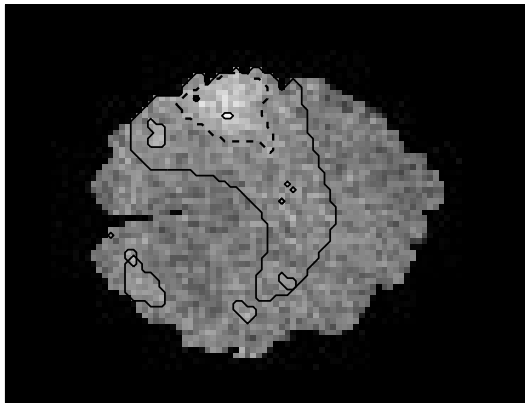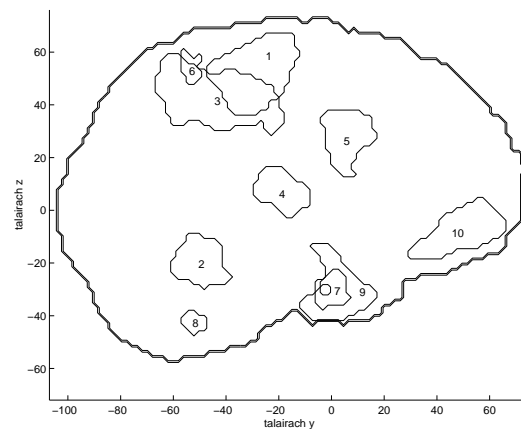
(a) Horizontal slice (z=56) of the contrast image with superimposed blobs. The slice is extracted through the most significant scale-space blob.
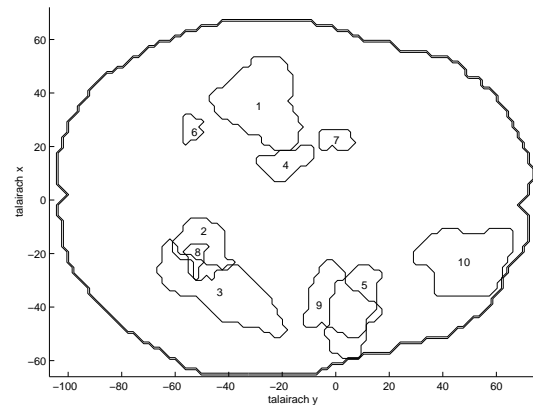
(b) Outline of the ten most significant scale-space blobs in the horizontal plane, viewed from above.
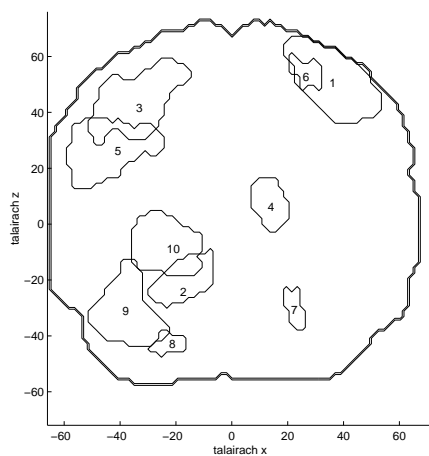
(c) Outline of the ten most significant scale-space blobs in the coronal plane, viewed from the front.

(d) Outline of the ten most significant scale-space blobs in the sagittal plane, viewed from the subjects right side.

Figure 9: The ten most significant blobs from the forced choice discrimination test, analyzed by 3D scale-space primal sketch with *absolute* base level, here shown in sagittal, coronal and horizontal cuts.

(a) Horizontal slice (z=56) of the contrast image with superimposed blobs. The slice is extracted through the most significant scale-space blob.

(b) Outline of the ten most significant scale-space blobs in the horizontal plane, viewed from above.
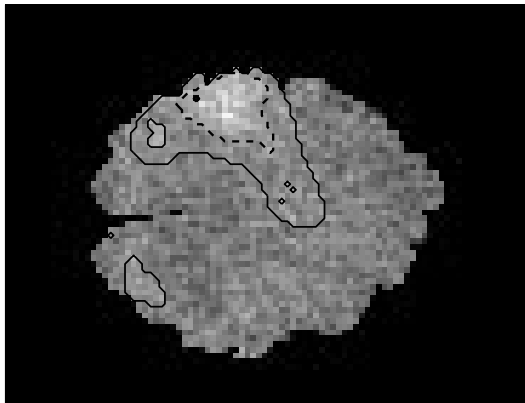
(c) Outline of the ten most significant scale-space blobs in the coronal plane, viewed from the front.
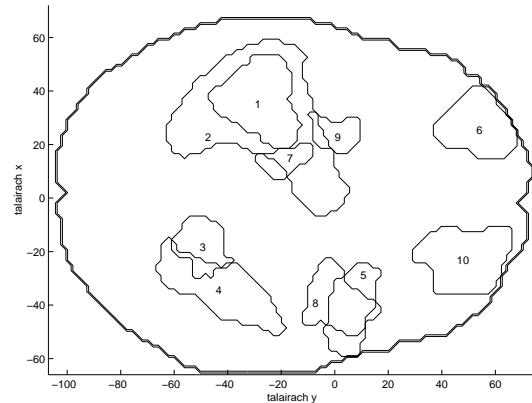
(d) Outline of the ten most significant scale-space blobs in the sagittal plane, viewed from the subjects right side.
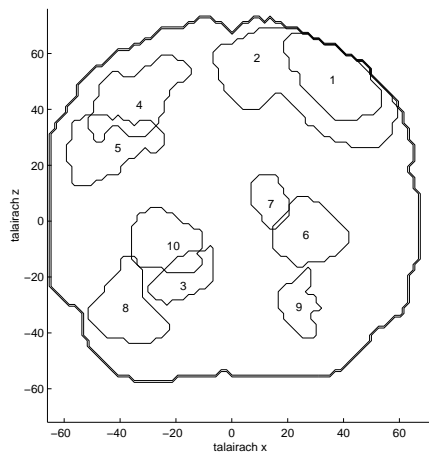
Figure 10: The ten most significant blobs from the forced choice discrimination test, analyzed by 3D scale-space primal sketch with *relative* base level, here shown in sagittal, coronal and horizontal cuts.
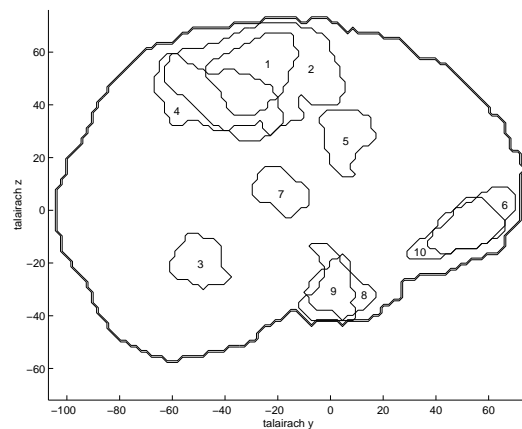
Index abs	Sign	Scale	Position	Vol mm³	Prev. sig	Index rel	Sign rel	D_i	Region name
1	1214.42	1.65	(36, -28, 56)	12016	yes	1	1450.10	-0.0747	L somatosensory and motor cortex
2	221.06	1.65	(-15, -52, -19)	3736	yes	3	224.18	-0.0037	R lobus anterior cerebellum
3	102.17	4.37	(-33, -42, 44)	11896	yes	4	102.67	0.0002	R interpareital sulcus
4	81.34	1.95	(12, -20, 10)	2000	yes	7	73.38	0.0471	L ventrolateral thalamus
5	61.10	2.49	(-49, 5, 30)	5992	yes	5	90.08	-0.1662	R middle frontal gyrus
6	57.50	0.42	(26, -54, 56)	408	yes	11	32.01	0.2567	L sup. pareital lobe
7	52.71	0.80	(22, 3, -29)	624	yes	9	62.72	-0.0732	L temporal pole
8	48.63	0.42	(-19, -54, -43)	368	yes	12	26.79	0.2613	R lobus posterior cerebellum
9	40.40	3.44	(-43, 3, -33)	5592	yes	8	65.34	-0.2064	R temporal pole
10	32.35	4.71	(-27, 55, -5)	6184	no	10	49.32	-0.1808	R superior frontal sulcus
11	32.28	3.44	(30, 53, -5)	5776	-	6	75.95	-0.3692	L superior frontal sulcus
12	31.73	1.08	(-19, -20, 64)	408	-	32	14.30	0.3485	L gyrus precentralis.
13	31.43	3.16	(22, -48, -23)	3176	-	27	15.34	0.3139	L lobus ant. cerebelli
14	29.09	1.02	(8, -54, 48)	552	-	15	22.45	0.1148	L sup. parietal sulcus
15	25.89	1.45	(-35, -42, 46)	488	-	59	9.86	0.4216	R intraparietal sulcus

Table 6: Table of the the fifteen most significant blobs from the forced choice discrimination test analyzed with *absolute* base level. The columns are; (Index abs) blob ranking, (Sign) scale-space significance, (Scale) scale of the scale-space blob, (Position) position in Talairach coordinates, (Vol) volume of the scale-space blob support region, (Prev. Sig) if the blob was previously regarded as significant according to (Roland et al., 1993), (Index rel) index of corresponding relative blob, (Sign rel) significance of corresponding relative blob, (D_i) measure of the change of significance according to section 3.6 and (Region name) name of activated region. The location and shape of the blobs can be viewed in figure 9. (The dashes '—' in rows 11-15 in column 'Prev sig.' indicate that these data are not available to us. (unpublished))

Index rel	Sign	Scale	Position	Vol mm³	Prev. sig	Index abs	Sign abs	D_i	Region name
1	1450.10	1.65	(36, -28, 56)	12016	yes	1	1214.41	-0.0496	L somatosensory and motor cortex
2	512.79	10.25	(38, -28, 54)	49680	yes	16	25.10	1.1836	L sup- pre-motor and som-sensory cor.
3	224.18	1.65	(-15, -52, -19)	3736	yes	2	221.06	-0.1205	R lobus anterior cerebellum
4	102.67	4.37	(-33, -42, 44)	11896	yes	3	102.17	-0.1245	R interpareital sulcus
5	90.08	2.49	(-49, 5, 30)	5992	yes	5	61.10	0.0420	R middle frontal gyrus
6	75.95	3.44	(30, 53, -5)	5776	no	11	32.28	0.2451	L superior frontal sulcus
7	73.38	1.95	(12, -20, 10)	2000	yes	4	81.34	-0.1713	L ventrolateral thalamus
8	65.34	3.44	(-43, 3, -33)	5592	yes	9	40.40	0.0821	R temporal pole
9	62.72	2.22	(22, 3, -29)	2176	yes	7	52.71	-0.0511	L temporal pole
10	49.32	4.71	(-27, 55, -5)	6184	no	10	32.35	0.0565	R superior frontal sulcus
11	32.01	0.42	(26, -54, 56)	408	-	6	57.50	-0.3810	L sup. parietal lobe
12	26.79	0.42	(-19, -54, -43)	368	-	8	48.63	-0.3856	R lobus posterior cerebellum
13	26.40	2.31	(48, -62, 2)	2416	-	17	23.92	-0.0838	L inferior temporal gyrus
14	23.19	0.86	(46, 39, -11)	560	-	30	15.88	0.0378	L inferior temporal gyrus
15	22.45	1.02	(8, -54, 48)	552	-	14	29.09	-0.2392	L sup. parietal sulcus

Table 7: Table of the ten most significant blobs from the forced choice discrimination test analyzed with *relative* base level. The columns are; (Index_rel) blob ranking, (Sign) scale-space significance, (Scale) scale of the scale-space blob, (Position) position in Talairach coordinates, (Vol) volume of the scale-space blob support region, (Prev. Sig) if the blob was previously regarded as significant according to (Roland et al., 1993), (Index_abs) index of corresponding absolute blob, (Sign abs) significance of corresponding absolute blob, (D_i) measure of the change of significance according to section 3.6 and (Region name) name of activated region. The location and shape of the blobs can be viewed in figure 10. (The dashes '−' in row 11-15 in column 'Prev sig.' indicate that these data were not available to us (unpublished).)

Forced choice discrimination experiment. This experiment was previously reported in (Ledberg et al., 1999). The study consists of six test subjects, performing one test condition and one rest condition with four repetitions of every condition. The test condition consisted of discrimination between objects of oblonged shape.

The PET images were realigned within subjects and reformatted to standard format using the human brain atlas of (Roland et al., 1994). There was no prefiltering of the data. These preprocessed images formed the input data to the general linear model, described in section 2.1. Nine parameters were used in the model: one for the mean, two for the different test conditions and six for the test subjects.

The residual noise from the tactile visual experiment was used for estimating the noise in the PET-images. From the $\varepsilon_i(x)$ images, a number of synthetic noise images were derived through a process described in (Ledberg, 1999). The synthetic noise images were used to estimate $V_m(t)$, $V_\sigma(t)$ and $\tau_{eff}(t)$ in the scale-space primal sketch.

The contrast derived from the GLM model was the test condition contrasted against the rest condition. The contrast image was analyzed in 3-D with the scale-space primal sketch. Multiple responses were merged and a mask was applied to remove blobs outside the brain.

Results. The result of the analysis when using an absolute base level can be seen in figure 9 and in table 6. For corresponding results using a relative base level, see figure 10 and table 7. With a relative base level, all the top ten ranked blobs have a larger support volume than 2000 mm^3 compared to using an absolute base level where blobs number 6 to 8 have a support volume of less than 1000 mm^3. Also, the blob ranked as number 2 when using relative base level with a support volume of 49680 mm^3 is not among the 15 most significant blobs when using an absolute base level. The matches between the support regions were perfect in all cases except one, where the support regions overlapped but had different spatial extent. The matching was done with the 100 most significant scale-space blobs in both the absolute and the relative cases and the match is the best possible among those.

The blobs have been compared to the significant regions found when using the method described in (Roland et al., 1993). When using absolute base level, blob number 10 was not regarded as significant. When using relative base level, blobs number 6 and 10 were not regarded as significant.

5   Summary and discussion

We have presented a comparison of using two different significance measures in the scale-space primal sketch applied on functional brain images. The original approach of using a relative base level was compared to new proposed absolute base level, and the purpose of this study was to investigate how this change affects the scale-space blob significance on PET contrast images as well as to what extent this influences the relative ranking of the blobs.

The experiments indicate that an absolute base level gives a higher degree of correspondence to an existing statistical method than using the relative base level. The statistical method uses the existence of a global zero level, which is one assumption underlying the argument for an absolute base level in the scale-space primal sketch. On the other hand, this imposes a stronger assumption about stationarity of the signal, which would be weaker when using a relative base level. In general the scale-space primal sketch gives biologically meaningful responses when the position of the blobs were compared to previously published brain activations in identical test setups (Seitz

et al., 1991), (Hadjikhani and Roland, 1998).

In the experiment in section 4.2 and the first experiment presented in section 4.3, it was noted that small blobs superimposed on the visual cortex were assigned a higher significance when using an absolute base level. Since the blobs were superimposed on larger activations they gained significance by adding the intensity of the larger activation to their significance values. In the forced choice experiment presented in section 4.3, it was noted that the absolute base level emphasizes small scale-space blobs, while the relative base emphasizes large scale-space blobs in term of size of support-region. It is a common phenomenon that small activations are superimposed on larger ones. These small activations gain more significance by using absolute base level than larger sized activations. Thus, changing the base level to an absolute will in general give a greater emphasis to smaller blobs relative to larger ones.

We have also presented a post-processing tool to the scale-space primal sketch for merging multiple scale-space responses corresponding to the same activation. This tool has been useful to give a better correspondence between activation strength and the significance of the scale-space blobs. This tool removes the need for choosing a scale-space blob to represent an activation when multiple scale-space blob represent the same activation and it also gives a more distinct difference between the significance of blobs corresponding to an activation and blobs corresponding to noise.

Moreover, we presented a new approach for collecting reference statistics for scale normalization, using residual noise images from the general linear model.

References

Björkman, E., Lindeberg, T. and Roland, P. E. (1999). In preparation.

Coulon, O., Bloch, I., Frouin, V., and Mangin, J.-F. (1996). The structure of PET activation maps, *Proc. 3rd International Conference on Functional Mapping of the Human Brain*, Copenhagen, Denmark. Neuroimage vol. 5 no. 4 p 391, 1997.

Coulon, O., Bloch, I., Frouin, V. and Mangin, J.-F. (1997). Multi-scale measures in linear scale-space for characterizing cerebral functional activations in 3D PET difference images, *in* B. M. ter Haar Romeny, L. M. J. Florack, J. J. Koenderink and M. A. Viergever (eds), *Scale-Space Theory in Computer Vision: Proc. First Int. Conf. Scale-Space'97*, Vol. 1252 of Springer verlag LNCS, Utrecht, The Netherlands, pp. 188–199.

Florack, L. M. J. (1997). *Image Structure*, Series in Mathematical Imaging and Vision, Kluwer Academic Publishers, Dordrecht, Netherlands.

Friston, K. J., Frith, C. D., Liddle and Frackowiak, R. S. J. (1991). Comparing functional PET images: The assessment of significant change, *J Cereb Blood Flow Metab* **11**: 81–95.

Friston, K. J., Worsley, K. J., Frackowiak, R. S. J., Mazziotta and Evans, A. C. (1994). Assessing the significance of focal activations using their spatial extent, *Human Brain Mapping* **1**: 210–220.

Hadjikhani, N. and Roland, P. (1998). Cross-modal transfer of information between the tactile and the visual representations in the human brain — A PET study, *J. of Neuroscience* **18**: 1072–1084.

Holmes, A. P., Blair, R. C., Watson, J. D. G. and Ford, I. (1996). Non-parametric analysis of statistical images from functional mapping experiments, *J Cereb Blood Flow Metab* **16**: 7–22.

Koenderink, J. J. (1984). The structure of images, *Biological Cybernetics* **50**: 363–370.

Ledberg, A. (1999). Robust estimation of the probabilities of 3D clusters in functional brain images: Application to PET data, *Human Brain Mapping* . in press.

Ledberg, A., Åkerman, S. and Roland, P. (1999). Estimation of the probabilities of 3-D clusters in functional brain images, *NeuroImage* **8**: 113–128.

Lidberg, P., Lindeberg, T. and Roland, P. (1996). Analysis of brain activation patterns using a 3-D scale-space primal sketch, *Proc. 3rd International Conference on Functional Mapping of the Human Brain*, Copenhagen, Denmark, p. 393. Neuroimage vol. 5 no. 4 p 393, 1997.

Lindeberg, T. (1993). Detecting salient blob-like image structures and their scales with a scale-space primal sketch: A method for focus-of-attention, *International Journal of Computer Vision* **11**(3): 283–318.

Lindeberg, T. (1994). *Scale-Space Theory in Computer Vision*, The Kluwer International Series in Engineering and Computer Science, Kluwer Academic Publishers, Dordrecht, the Netherlands.

Lindeberg, T. (1998). Feature detection with automatic scale selection, *International Journal of Computer Vision* **30**(2): 77–116.

Lindeberg, T., Lidberg, P. and Roland, P. (1999). Analysis of brain activation patterns using a 3-D scale-space primal sketch, *Human Brain Mapping* **7**(3): 166–194.

Poline, J.-B. and Mazoyer, B. (1993). Cluster analysis in individual functional brain images: Some new techniques to enhance the sensitivity of activation detection methods, *J Cereb Blood Flow Metab* **13**: 425–437.

Roland, P. E. (1993). *Brain Activation*, John Wiley and Sons, New York.

Roland, P. E., Graufelds, J., Wåhlin, J., Ingelman, L., Andersson, M., Ledberg, A., Pedersen, J., Åkerman, S., Dabringhaus, A. and Zilles, K. (1994). Human brain atlas: For high-resolution functional and anatomical mapping, *Human Brain Mapping* **1**: 173–184.

Roland, P. E., Levin, B., Kawashima, R. and Åkerman, S. (1993). Three-dimensional analysis of clustered voxels in ^{15}O-butanol brain activation images, *Human Brain Mapping* **1**: 3–19.

Searle, S. (1971). *Linear models*, Wiley, New York.

Seitz, R., Roland, P., Bohm, C., Greitz, T. and Stone-Elander, S. (1991). Somatosensory discrimination of shape-tactile exploration and cerebral activation, *Eur. J. Neurosci.* **3**: 481–492.

Witkin, A. P. (1983). Scale-space filtering, *Proc. 8th Int. Joint Conf. Art. Intell.*, Karlsruhe, West Germany, pp. 1019–1022.

Worsley, K. J., Evans, A. C., Marrett, S. and Nelin (1992). A three-dimensional analysis for CBF activation studies in human brain, *J. Cereb. Blood Flow Metab.* **12**: 900–918.

Worsley, K. J., Marret, S., Neelin, P. and Evans, A. C. (1996b). Searching scale space for activation in PET images, *Human Brain Mapping* **4**: 74–90.